第二章：扫描隧道谱及其应用

吴克辉
中科院物理所

扫描隧道谱的典型应用：

1. 半导体（元素、化合物）表面电子态
2. 半导体中的掺杂原子的分布和电离
3. 量子限域结构(2D\1D\0D)中的分立电子态
4. 表面电子驻波(Electron standing wave)
5. 电荷密度波(CDW)/表面相变
6. Kondo效应
7. 库仑阻塞
8. 单分子隧道谱/单分子操纵
9. 超导体的电子态
10. 表面磁结构/单自旋/自旋密度波
11. 复杂氧化物表面
12. 超薄绝缘体/分子吸附体系
13. 二维电子体系（graphene\拓扑绝缘体）

。。。

2.1 扫描隧道谱的基本原理和技术

- 一般原理
- 不同种类
- 实施技术要点

§ 2-1 STS原理

“满态”像和“空态”像

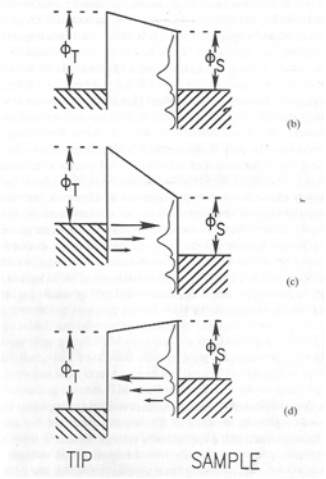

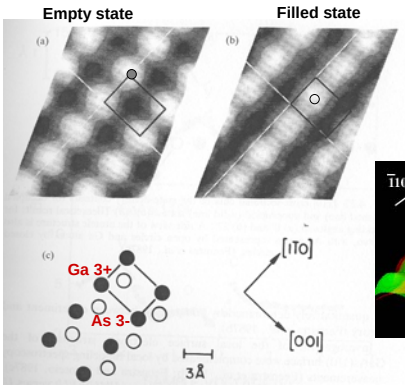

GaAs(110)

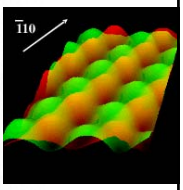

Fig. 4.26. Constant-current STM images of the GaAs(110) surface acquired at sample bias voltages of (*a*) +1.9 V and (*b*) −1.9 V. (*c*) Top view of the surface atoms. The As atoms are represented by open circles and the Ga atoms by closed circles. The rectangle indicates a unit cell, whose position is the same in all three figures (Feenstra *et al.*, 1987b).

?是否可以认为满态像反应了电子占据态的空间分布，而空态像反应了电子空态的空间分布？

偏压依赖像（Bias-dependent STM imaging）

GaN(0001)表面的两种主要再构

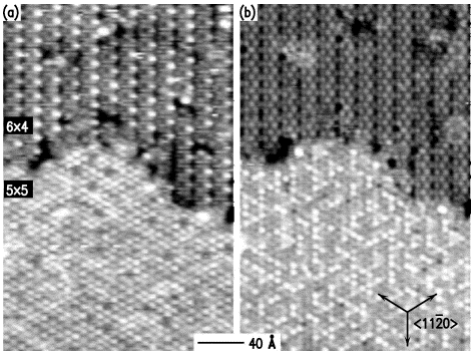

empty states +1.0 V　　filled state −1.0 V

Dual bias images of the 5×5 and 6×4 reconstructions. The average height difference between the two reconstructions is 0.3 Å for empty states (+1.0 V sample voltage) shown in (a) and 0.4 Å for filled states (−1.0 V sample voltage) shown in (b), with the 5×5 being higher in each case. In both images, the total gray scale range is about 1.3 Å. ***A. R. Smith et al. Surf. Sci. 423, 70(1999)***

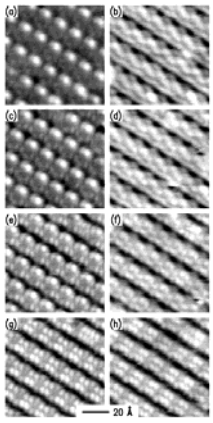

Simultaneously acquired dual bias images of the 6×4 reconstruction. Sample biases are +2.0 and −2.0 V for (a) and (b), +1.5 and −1.5 V for (c) and (d), +1.0 and −1.0 V for (e) and (f), and +0.5 and −0.5 V for (g) and (h), respectively. Similarly, gray-scale ranges are 1.1 and 0.7 Å for (a) and (b), 1.1 and 0.8 Å for (c) and (d), 1.1 and 0.9 Å for (e) and (f), and 1.3 and 1.3 Å for (g) and (h).

主要缺点：难以把形貌和电子态密度信息分开

什么是扫描隧道谱？

Scanning tunneling spectroscopy

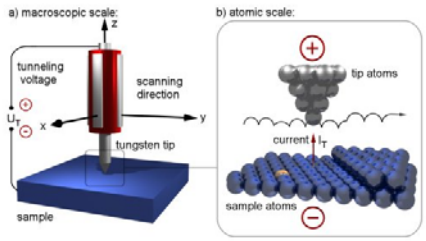

I = I(x, y, z, V)

STM实验中有(x,y,z,V,I)五个变量。
通常扫描图象时常保持V恒定。
测量I(V)谱（扫描隧道谱STS)时，V是变化的。

STM的工作模式

- 恒流模式(V,I)=const. (x,y)/z,测量电子态的空间分布
- 等高模式(V,Z)=const. (x,y)/I,测量态的分布与贡献
- 恒阻模式
- 可变间距模式
- 恒定平均电流模式

STM不仅是原子分辨和原子操控的工具，
从I对(x,y,z,V)的依赖关系中，可以分析出许多谱学信息，
结合STM的原子分辨功能，使STM成为强大的单原子尺度的谱学工具。

§ 2-2扫描隧道谱的不同形式(x, y, z, V)

- 扫描隧道谱 （STS）
  - 电压电流谱（I(V)） **I = I(x, y, z, V)**
    - 微分电导谱（dI/dV(V)）
      dI/dV 成像
      CITS像
    - 二次微分谱(非弹性隧道谱) $d^2I/dV^2(V)$
      $d^2I/dV^2(V)$ 成像
  - I-Z谱
    局域功函数成像
  - I-t谱

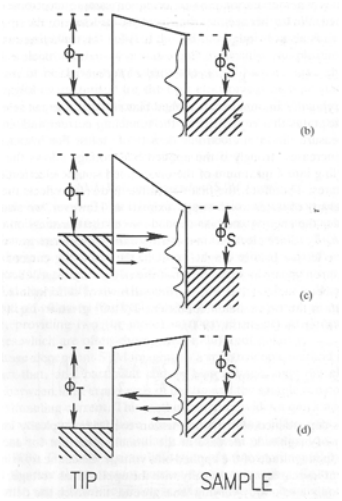

隧道电流随针尖-样品之间的偏压变化情况

当样品是金属（费米能级位于能带中间，费米能级附近的电子态密度变化不剧烈），并且针尖和样品之间施加的电压比较小（mV量级）的时候，隧道电流与电压呈线性关系。

$$I \propto \rho_s(E_F)\cdot eV$$

当电压较高，或者样品是半导体(电子态密度的变化比较剧烈)的时候，这种线性关系一般不再成立。所以STM图像通常会随电压变化呈现明显的变化。研究这种变化能够得到不同的电子谱，并且结合STM的原子分别能力，获得原子分辨的电子谱（Hamers, Tromp, Feenstra等人在1990前后发展）。

隧道电流与电压的一般关系

隧道电流电压微分谱 dI/dV （V）

$$I=(\frac{2\pi e}{\hbar})\int_{-\infty}^{\infty}|M|^2\,\rho_t(E)\rho_s(E+eV)[f(E)-f(E+eV)]dE$$

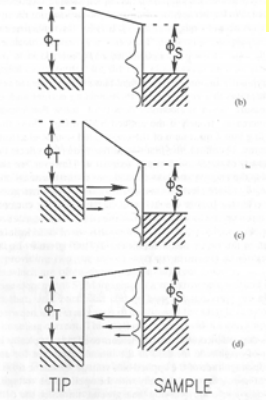

对于 kT～0时，一般情况：

$$I\propto\int_0^{eV}|M|^2\,\rho_t(E)\rho_s(E+eV)dE$$

$$\frac{dI}{dV}\propto|M|^2\,\rho_t(0)\rho_s(eV)+\int_0^{eV}\rho_t(E-eV)\rho_s(E)\frac{d|M|^2}{dV}dE$$

$$\frac{dI}{dV}\propto\rho_s(eV)$$

☛在很多情况下，针尖态密度和矩阵元都可以近似为常数，***dI/dV***谱就直接反映出了样品的态密度信息。**STM**探针所据有的原子级的空间分辨，使得***I-V*** 谱或***dI/dV***谱可以用以检测局域的具有空间分辨的电子态密度信息。

固定高度，单点电导*I(V)*与微分电导*dI/dV*谱

反馈回路关闭！

（1）数值微分方法：直接对***I-V***谱通过数值微分获得

（2）锁相放大技术：通过加适当频率的小电压正弦调制信号，即在偏压上叠加Δ***V*** 的正弦信号，测量电流的变化量Δ***I***，从而直接获得***dI/dV***

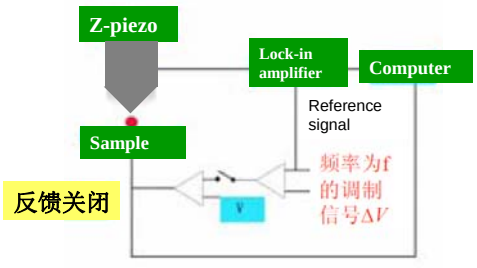

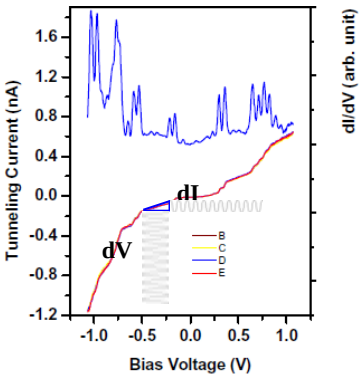

STS谱测量中的锁相技术

振幅为 ΔV、频率为 f 的正弦调制信号，引起电流信号产生 ΔI 的响应

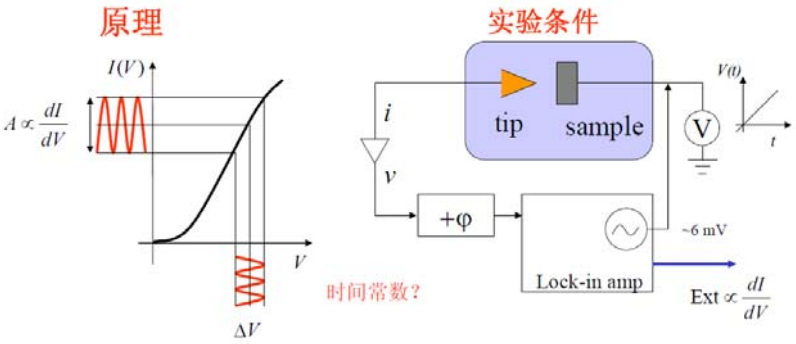

恒定电流微分电导(*dI/dV*)像（STS at constant current）

I = I(x, y, z, V)

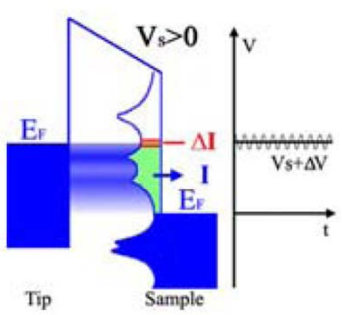

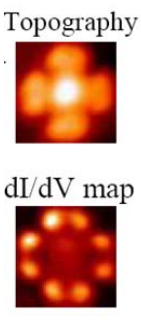

- 在使用恒流模式获得STM图像的同时，在电压信号上叠加一个微小的调制信号dV，使用锁相放大器检出相应的电流振荡信号dI，从而获得一副dI/dV(x,y)图像。
- 由于调制信号的频率高于针尖反馈的频率，所以STM形貌像不受影响。
- 这种模式适合于检测某个特定电子态的空间分布图像。

§ 2-2 应用举例

（1）量子限域效应造成的电子波结构

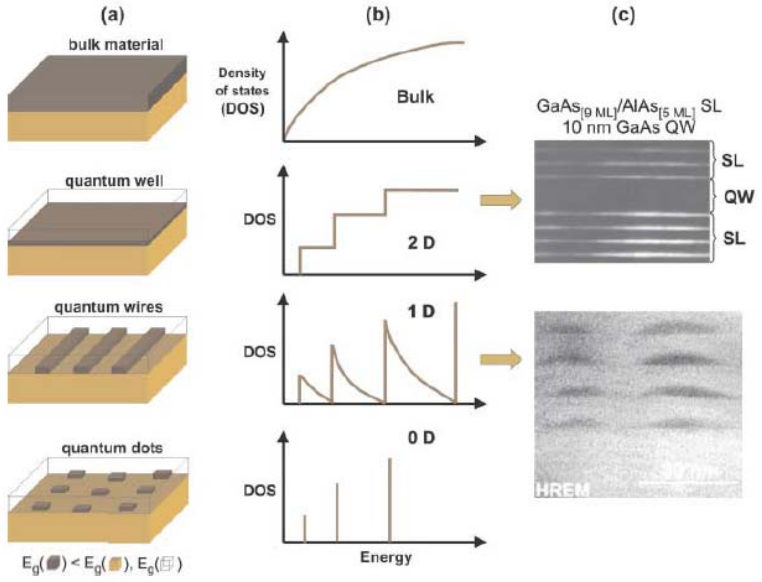

一维无限深势阱中的电子运动

For a string of length L only a specified number of wavelengths and frequencies are allowed.

$L = \frac{1}{2}\lambda n$

where n = 1, 2, 3.....

$\lambda_n = \frac{2L}{n}$

$f_n = \frac{v}{\lambda} = \frac{v}{2L}n$

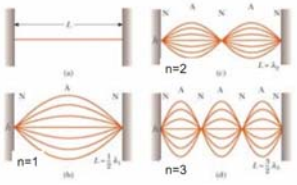

Formally solving the equation

$$-\frac{\hbar^2}{2m}\frac{d^2\psi(x)}{dz^2} = E\psi(x)$$

Within the well, subject to the boundary conditions
$\psi(z) = 0$ for $z < 0$ and $z > L_z$
The eigenfunctions are

$$\psi_n(x) = A_n \sin\left(\frac{n\pi x}{L}\right)$$

Where A_n is a normalization constant
The eigenenergies are

$$E_n = \frac{\hbar^2}{2m}\left(\frac{n\pi}{L}\right)^2$$

Index, n, is a (positive) integer, i.e., $n = 1\ 2\ ,3,\ldots$

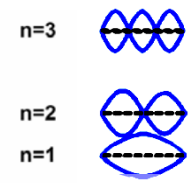

← 在x点发现电子的几率$\rho(x) \propto |\psi_n(x)|^2$

无限深势阱与有限深势阱的比较

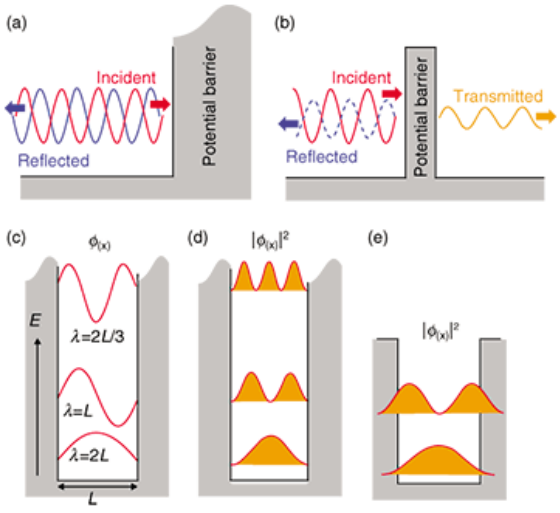

1 : 金属薄膜中的量子阱态
QWS in vertically confined metal films

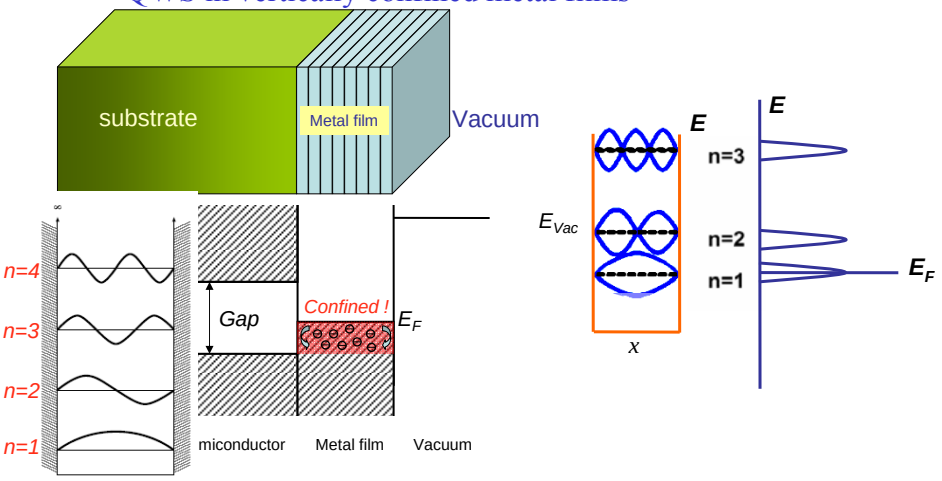

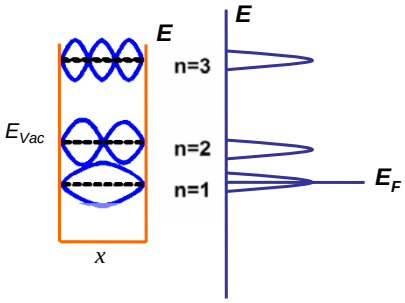

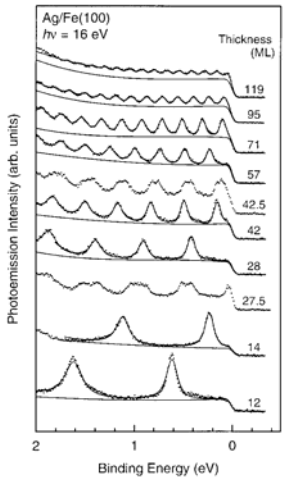

Normal emission spectra from quantum well states in epitaxial Ag films of varying thickness.

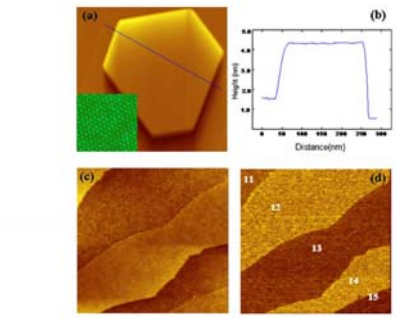

FIG. 1. (Color online) (a) STM image of a Pb island taken at $V=-0.8$ V and $I=0.1$ nA. Image size: 500×500 nm^2. Insert is a 5×5 nm^2 atomic resolution image ($V=0.4$ V, $I=0.1$ nA). (b) A line plot along the blue line in (a) to show the height profile. (c) The topographic and (d) local work function images taken simultaneously ($V=-2$ V, $I=0.1$ nA). The bright area has a larger work function than the dark area. Image size: 337×337 nm^2.

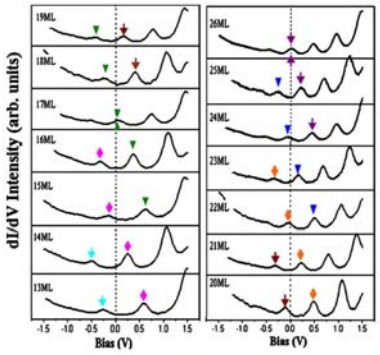

FIG. 3. (Color online) dI/dV curve of Pb films between $N=13$ and 26 ML (without counting the wetting layer). The measurement was done at $T=77$ K with sample bias ramp from -1.5 to 1.5 V. Same shape triangles are used here to indicate the shifts of the peak positions as a function of N, whereas upward triangles indicate the QWS peaks near the Fermi level.

Y. Qi et al, Appl. Phys. Lett. 90, 013109 (2007)

Notes:

1. 空态特征明显（对比PES满态特征）

2. 由于传统系数随电压变化导致的U型背景

dI/dV (x,y, V):
空间分辨 + 能量分辨

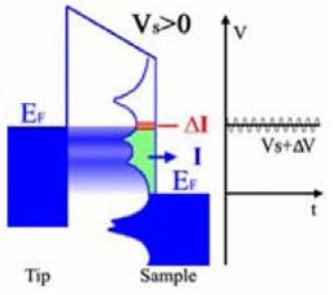

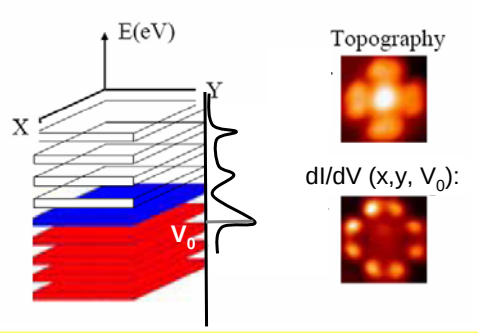

实际：在电压信号上叠加高频调制信号dV → dI，
使用锁相放大器直接读出
dI/dV(V)

固定偏压，对于平面上每一个点都采集$dI/dV(V_0)$，即得到二维$dI/dV(x,y,V_0)$ $\propto\rho$（E_F+eV_0）图。该图反应了样品E_F+eV_0能量处的态密度在空间的分布。改变偏压，即可得到对应样品不同能级的态密度在空间的分布。

dI/dV~V的关系曲线中可以辨认不同能量的本征态

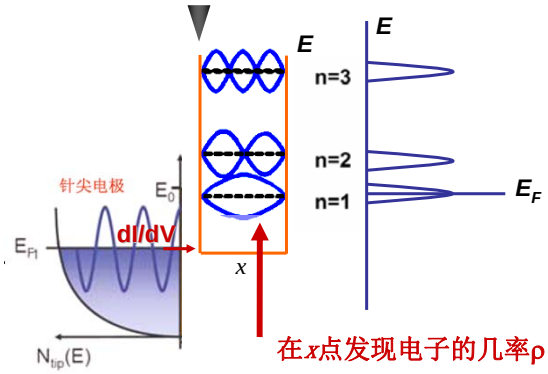

在x点发现电子的几率$\rho(x) \propto |\psi_n(x)|^2$

dI/dV (x, V): 空间分辨 + 能量分辨

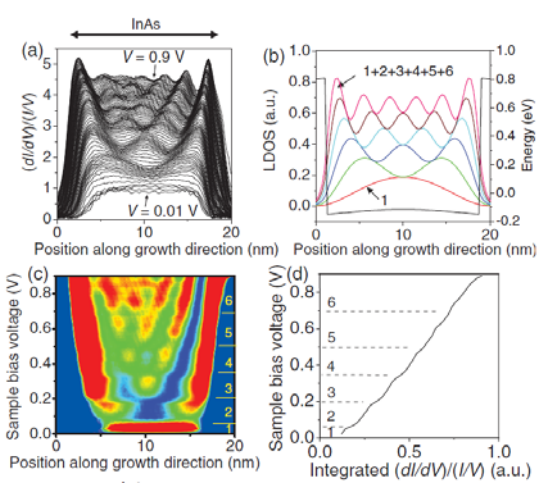

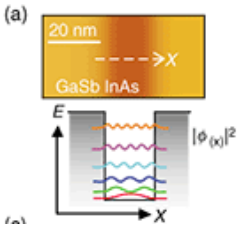

FIG. 3 (color). (a) High spatial and energy resolution STS spectra for 17 nm/23 nm QW, focusing on the white dotted circle in Fig. 2(c). $(dI/dV)/(I/V)$ curves are plotted for each V with a step of 0.01 V. (b) Calculated LDOS spectra taken to be the sum of the squared wave functions for subbands. The conduction band potential profile modulated by the electron accumulation in the well is overlaid. (c) Enhanced STS spectra. In the InAs layer, oscillation minima in $(dI/dV)/(I/V)$ curves as a function of the position along the growth direction at each V are set to zero. The subband indices are indicated. (d) Experimentally deduced electron density of states: each $(dI/dV)/(I/V)$ curve in (a) is integrated over the quantum well. (e) Enhanced STS spectra for 12 nm/15 nm QW. (f) STS spectra for 6 nm/7 nm QW.

K. Suzuki et al. PRL 98, 136802(2007)

3. 一维金属链中的量子阱态

Pd_{20} Chain

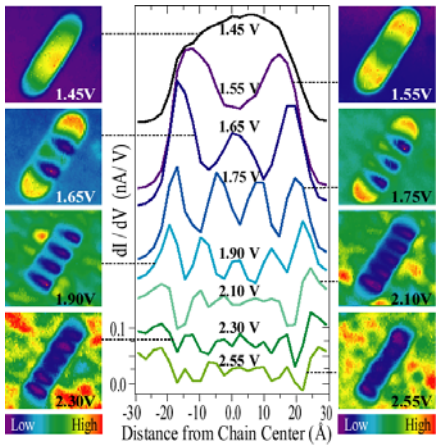

THE JOURNAL OF PHYSICAL CHEMISTRY B LETTERS
2005, *109*, 20657−20660
Published on Web 09/13/2005

Realization of a Particle-in-a-Box: Electron in an Atomic Pd Chain

N. Nilius,† T. M. Wallis,‡ and W. Ho*
Department of Physics and Astronomy and Department of Chemistry, University of California, Irvine, California 92697-4575

Received: June 27, 2005; In Final Form: July 28, 2005

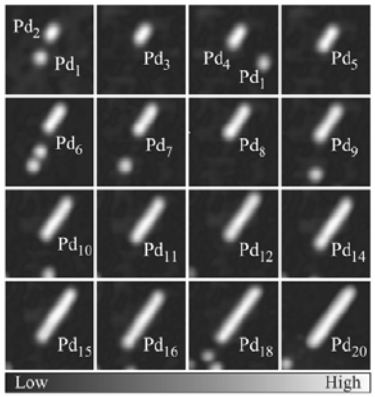

Figure 1. Assembly of individual Pd atoms to fabricate a Pd_{20} chain on NiAl(110), using atom manipulation techniques with the tunneling gap set at $V_{sample} = 2$ mV and $I = 45$ nA. The images were taken at $V_{sample} = 2.0$ V, $I = 1.0$ nA. Each image is 75 Å × 75 Å.

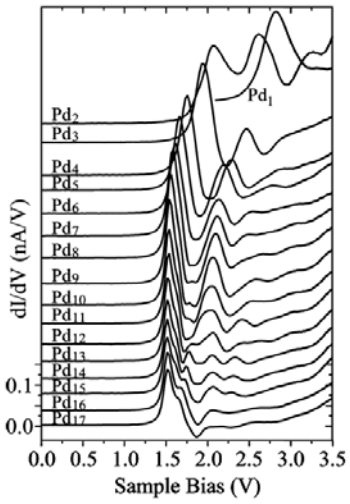

Figure 2. dI/dV spectroscopy of a single Pd atom and Pd chains containing between 2 and 17 atoms on NiAl(110). The gap was set with $V_{sample} = 3.0$ V, $I = 1.0$ nA. All spectra were taken in the chain center and are offset for clarity.

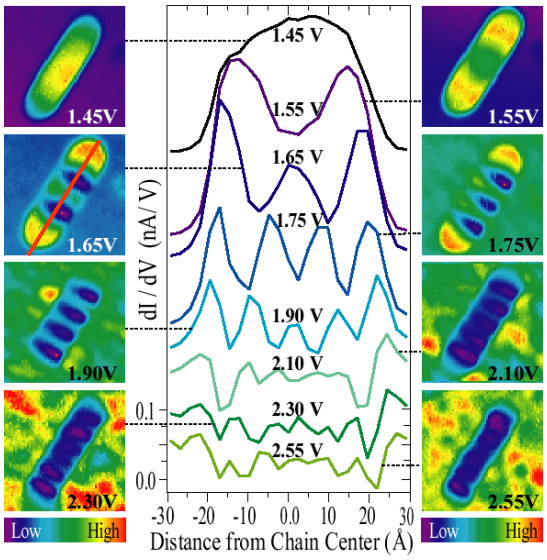

—“人工原子”

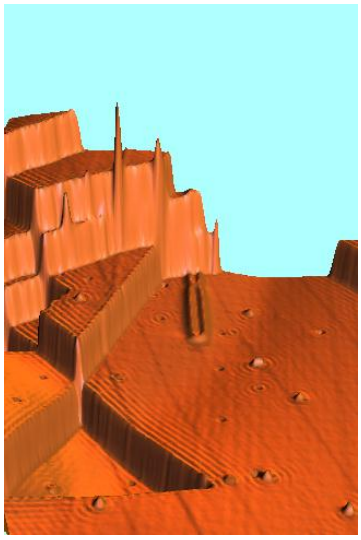

Copper Surface

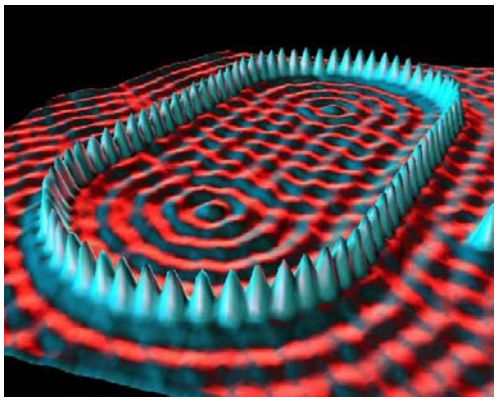

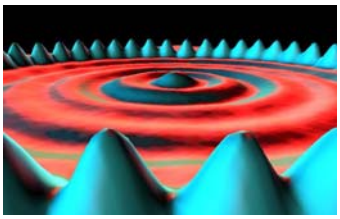

Iron on Copper

4. 量子点的电子波

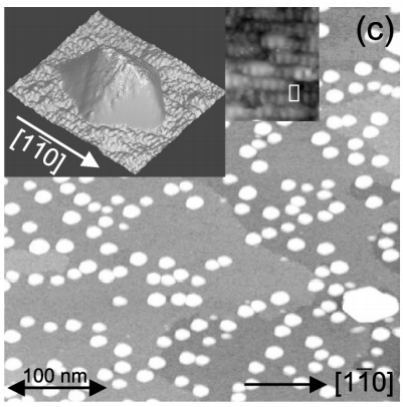

InAs QDs

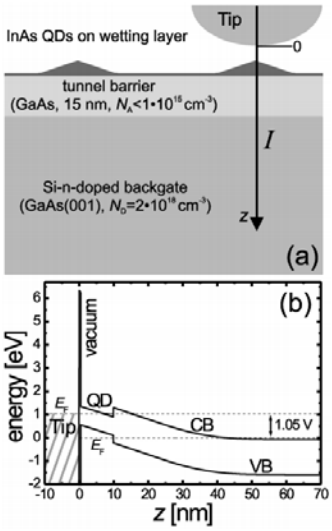

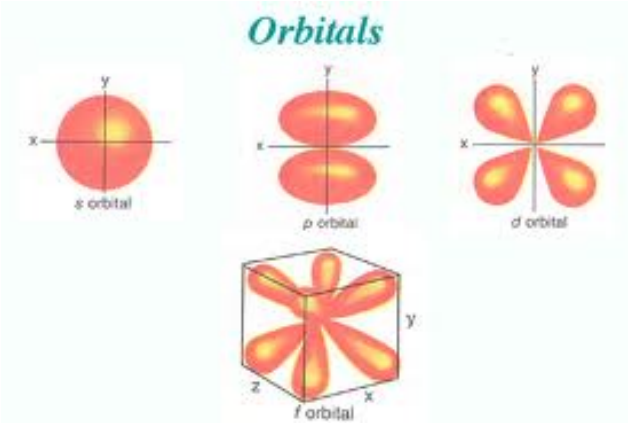

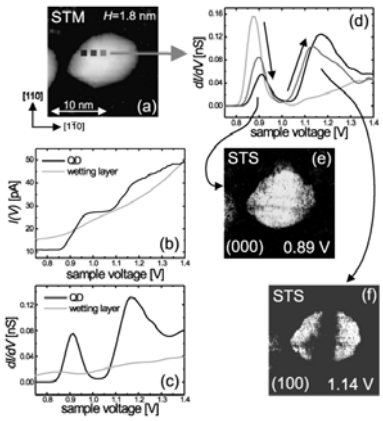

FIG. 2. Single QD, W tip: (a) constant-current image, V_{sample} = 1.7 V, I = 50 pA, height H and crystallographic directions marked; (b) $I(V)$ curves recorded on the QD (black line) and on the wetting layer (grey line), V_{stab} = 1.6 V, I_{stab} = 50 pA; (c) dI/dV curves recorded simultaneously with (b), V_{mod} = 28 mV; (d) dI/dV curves recorded at different positions above the QD as marked in (a); (e),(f) spatially resolved dI/dV data at V_{sample} = 0.89 V and V_{sample} = 1.14 V, respectively; all data in Fig. 2 are raw data.

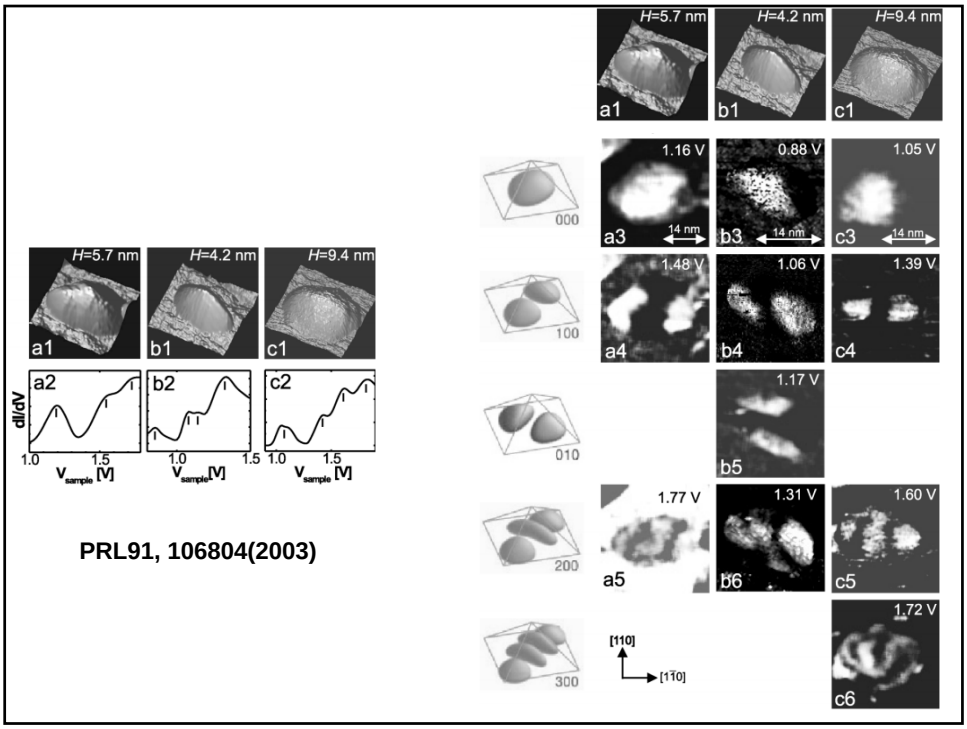

PRL91, 106804(2003)

§ 2-2 应用举例

（2）二维电子气的色散

Electron Waves

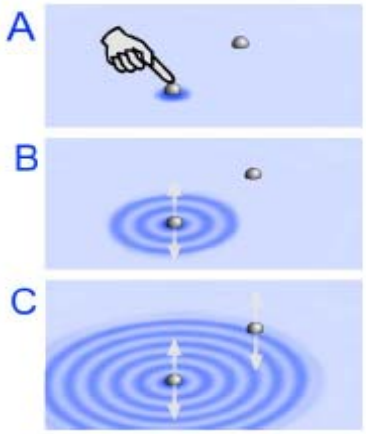

STM?

Electron Wave interference

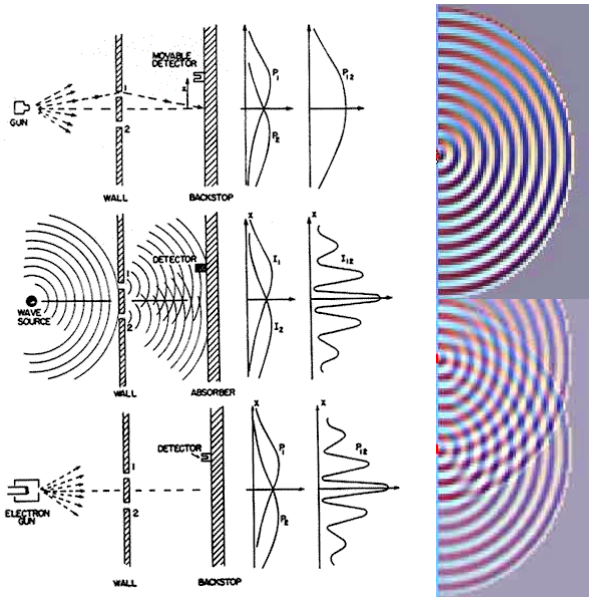

First direct probes of Standing Waves in Noble Metals (Au, Ag, Cu)

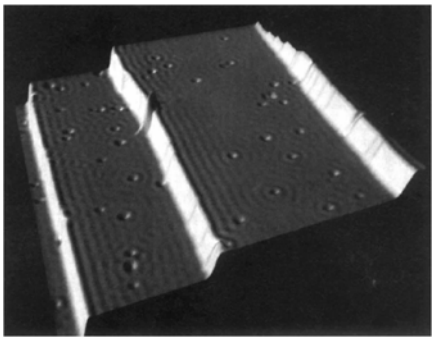

Cu(111)

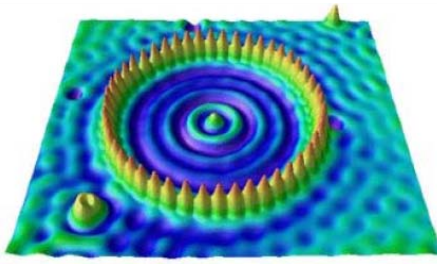

Fe atoms on Cu(111)

Crommie M F et al. Nature 363, 524(1993);
Crommie M F et al. Science 262, 218(1993);

Standing Waves on Other Metals and Semiconductors

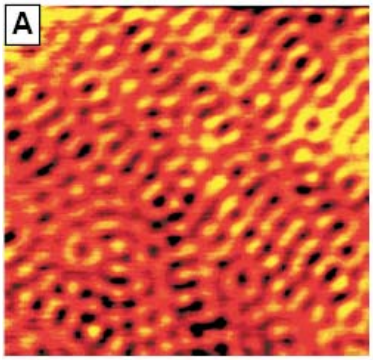

Be(0001)

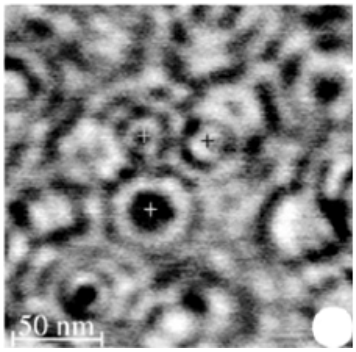

InAs(110)

Science 275, 1764(1997);
Phys. Rev. Lett. 81, 5616(1998);

经典二维电子气的色散

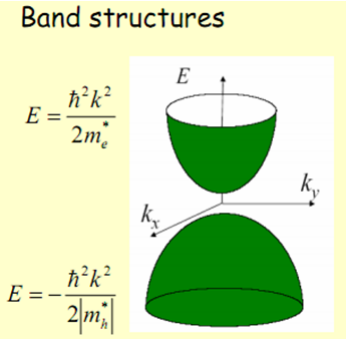

通过测量不同能量下准粒子驻波的波长大小，再结合式 λ =2π / ***q*** 与***q = k_f - k_i***，即可得出准粒子的能量色散关系。

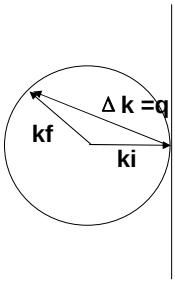

最可能的散射对应背散射
$\Delta k = 2k_i = 2 k_F$

Friedel 振荡的波长为
$\lambda = 2\pi /2k_i = \pi /k_F$

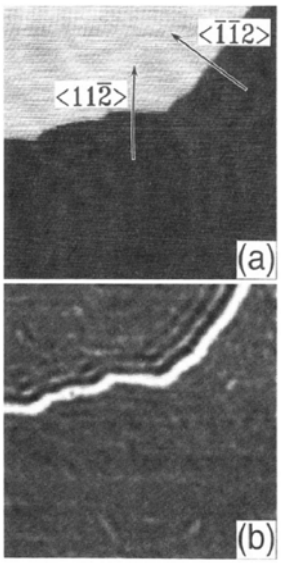

FIG. 1. (a) STM image of a Au(111) surface with a step. The size of the image is about 320 Å×320 Å. (b) Contrast image of the quantity $(dI/dV)/(I/V)$ calculated at +0.15 V from tunneling spectra obtained over the same area shown in the STM image of (a). The stabilizing bias voltage is −1 V.

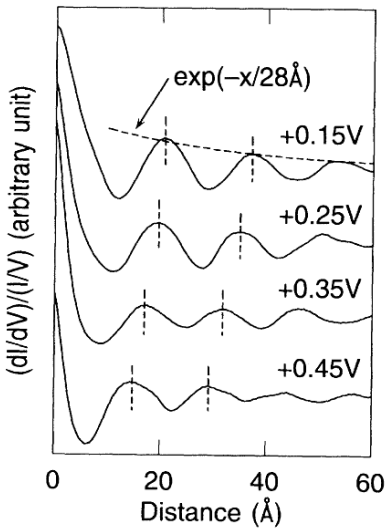

Y.Hasegawa, PRL 71, 1071(1993)

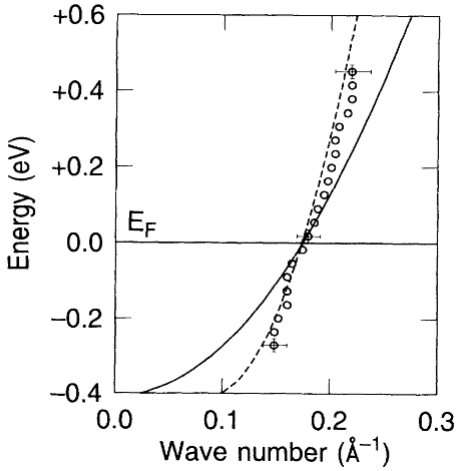

Y.Hasegawa, PRL 71, 1071(1993)

Ag(111)表面驻波

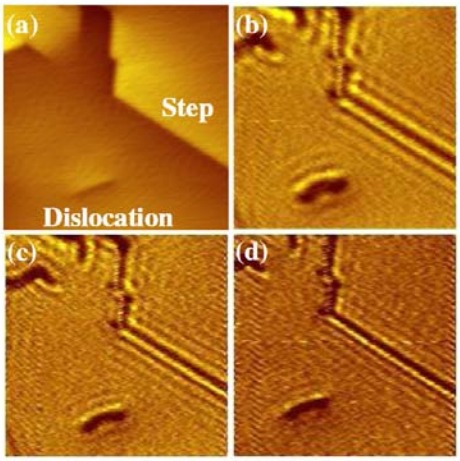

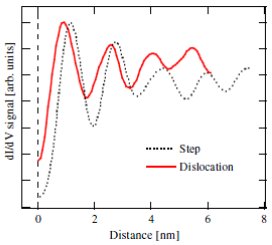

FIG. 1 (color online). (a) STM image and (b)–(d) dI/dV images of a 40 ML Ag(111) film surface. The tunneling current was 0.55 nA. Sample bias voltage was 0.20 V in (a) and (b), 0.30 V in (c), and 0.40 V in (d). Image size is 33.0 nm × 33.0 nm.

PRL 104, 016806 (2010)

graphene

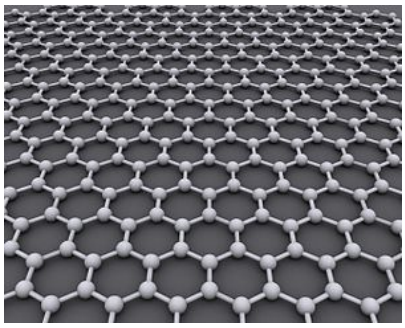

Graphene:
a single one-atom thick sheet of carbon atoms arranged in a honeycomb lattice

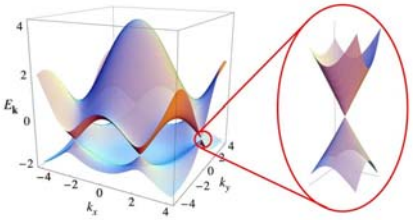

- **Massless Dirac Fermion:**
  1.Linear dispertion
  2.Pseudospin and chirality
- **Graphene is a topological insulator -QSHE**
  -But the SO gap is too small

Free-standing silicene sheet

Increased buckling – increased sp3 nature

sp2

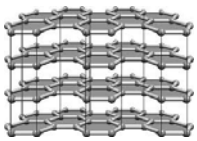

0.4 Å

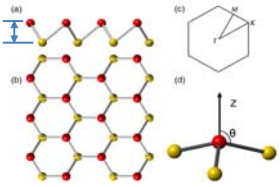

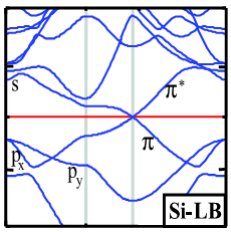

Dirac Fermion:
$V_F \sim 10^6$ m/s

sp3

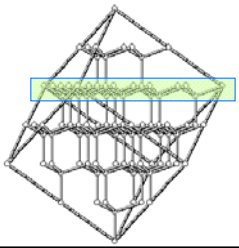

S. Cahangirov calculated the phonon spetrum of silicene and claimed that free-standing silicene is energetically stable

S. Cahangirov *et al.,* Phys. Rev. Lett. 102, 236804 (2009)

Advantages of silicene:
a comparison with graphene

- Stronger spin-orbit coupling
  - **– graphene (μeV) ->silicene (meV)**
  - **– True topological insulator**
- Easier to tune by electric field
  - **AB plans are shifted vertically**

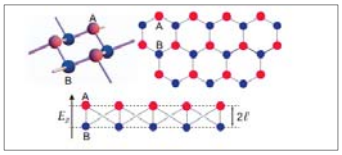

- Compatibility with Si technology
  - **High purity material**
  - **Easy doping**
  - **Si-based nano-fabrication**

G. G. Guzman-Verri et al. Phys. Rev. B 76, 075131 (2007)

S. Cahangirov et al., Phys. Rev. Lett. 102, 236804 (2009)

C. C. Liu et al, Phys. Rev. Lett. 107, 076802(2011)

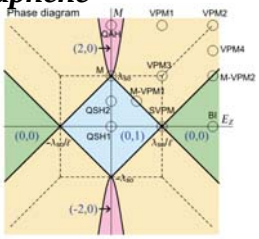

M. Ezawa *et al.*, **PRL**, 2012

Novel quantum effects

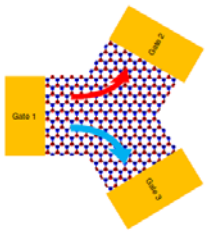

Tsai *et al*. **Nature Comm**. 2013

100% spin splitting

Experimental synthesis of silicene

Silicene on Ag(111)

4x4

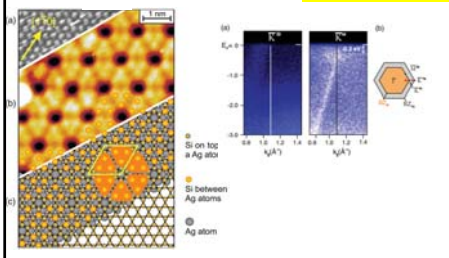

P. Vogt at al., Phys. Rev . Lett. 108, 155501 (2012)

4x4 √13x√13 √3x√3

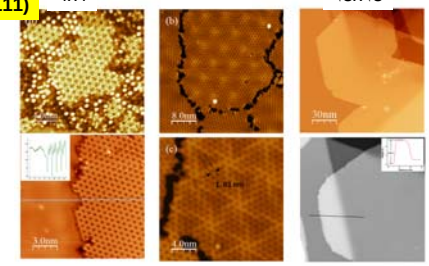

B. J. Feng et al. **Nano Lett.** 12, 3507(2012) **citation > 140**

Silicene on Ir(111)

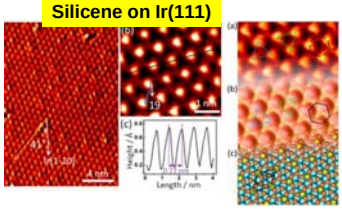

L. Meng et al. Nano Lett. 13, 685(2013)

Silicene on ZrB_2(111)

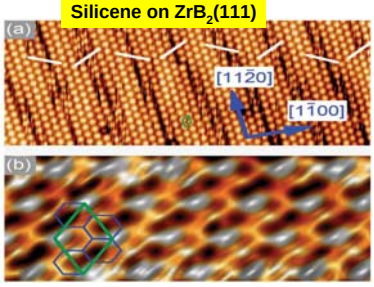

A. Fleurence et al., PRL 108, 245501 (2012)

Dirac Fermion versus conventional 2DEG

Band structures

Conventional 2D Electron System

$$E = \frac{\hbar^2 k^2}{2m_e^*}$$

$$E = -\frac{\hbar^2 k^2}{2|m_h^*|}$$

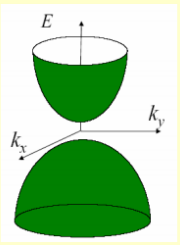

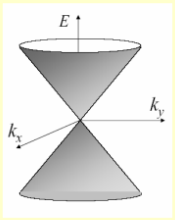

$$E = \hbar v_F |\vec{k}'_\perp|$$

Graphene

- Zero band mass
- Strict electron hole symmetry
- Electron hole degeneracy

4x4 √13x√13 √3x√3

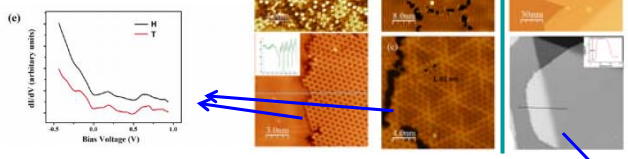

No QPI

B. J. Feng et al. Nano Lett. 12, 3507(2012)

QPI patterns

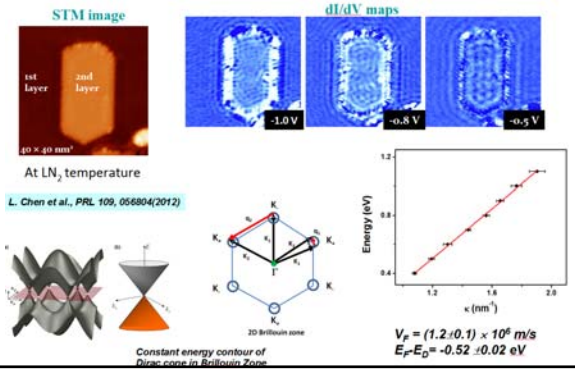

QPI from silicene steps

dI/dV maps

Line profiles

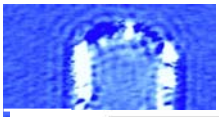

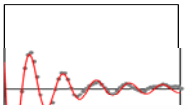

STM image

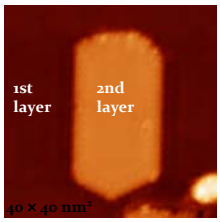

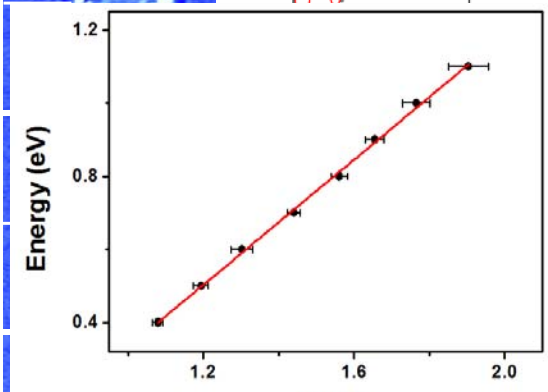

At LN_2 temperature

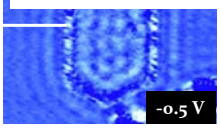

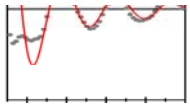

L. Chen et al., Phys. Rev. Lett. 109, 056804(2012).

Quasiparticle interference (QPI)

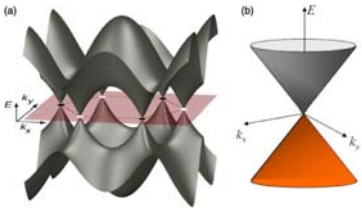

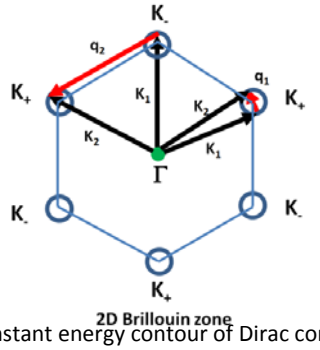

Constant energy contour of Dirac cone in Brillouin Zone

q_2: intervalley scattering

⇩

$(\sqrt{3} \times \sqrt{3})R30°$ interference pattern

q_1: intravalley scattering

⇩

Long wavelength standing wave

Scattering wave vector: $|q_1| = 2\kappa$, where κ is radius of constant-energy circles at K point

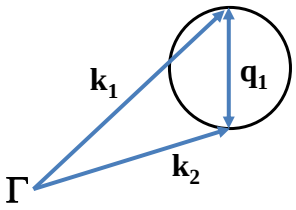

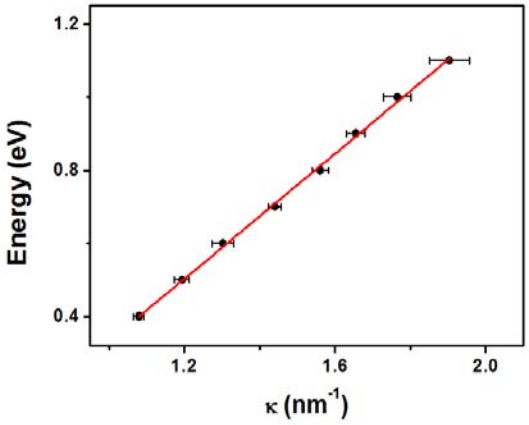

$V_F = (1.2 \pm 0.1) \times 10^6$ m/s

$E_F - E_D = -0.52 \pm 0.02$ eV

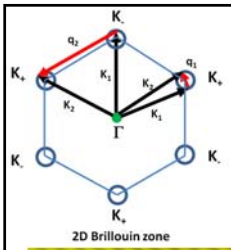

Intervalley scattering in silicene

$\sqrt{3} \times \sqrt{3}$ Interference pattern around point defects and step edges

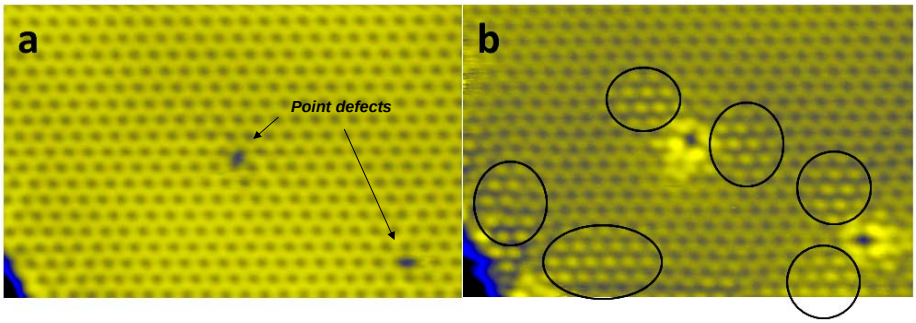

+ 1.3 V filled state

- 1.3 V empty state

Quasiparticle scattering patterns(QPI) on multilayer Si

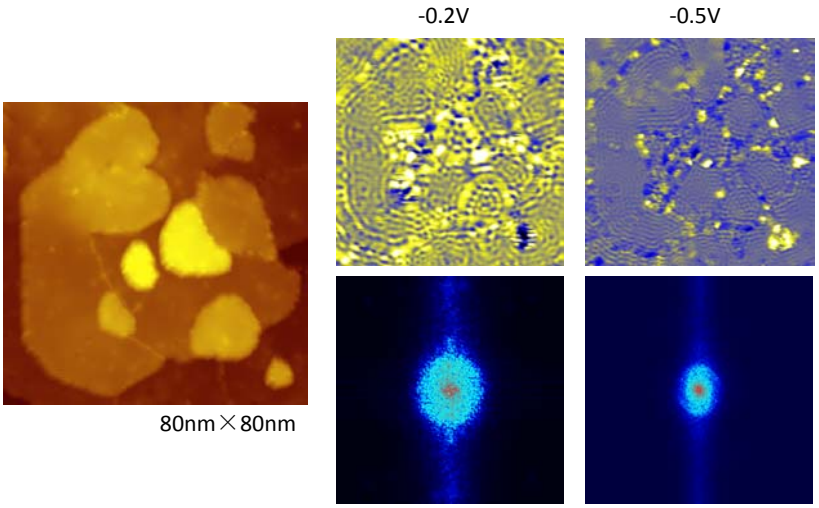

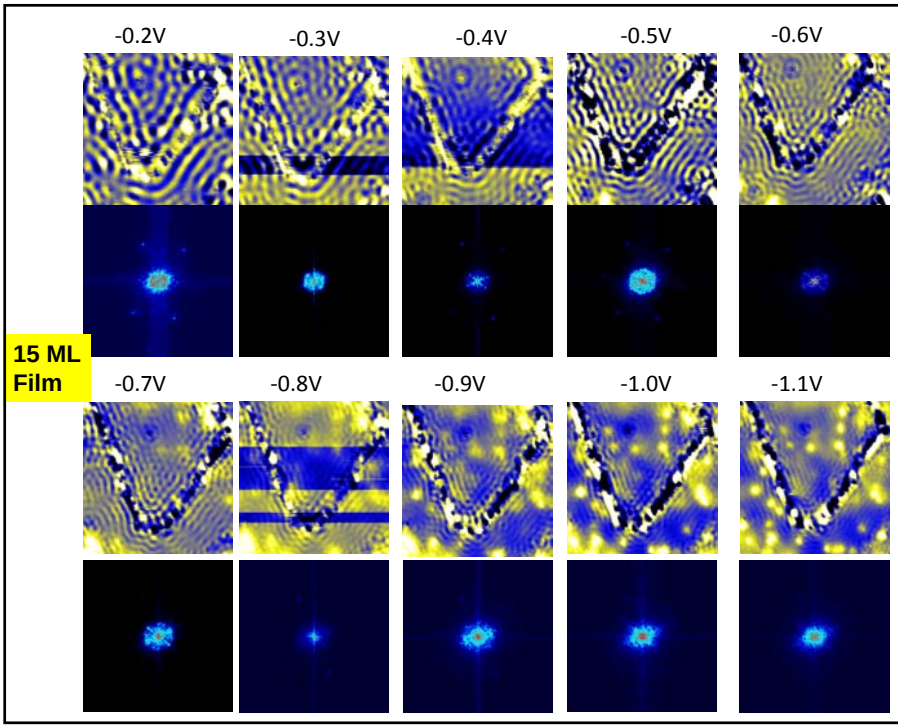

Dirac state persists on the surface

Standing Waves near armchair and zigzag edges.

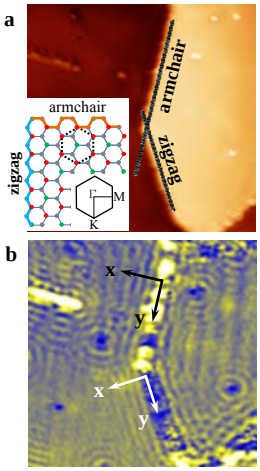

30ML film

STS measurement at 77 K

Linear E-k dispersions

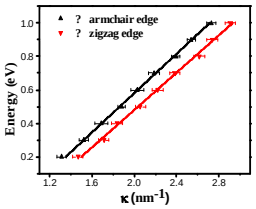

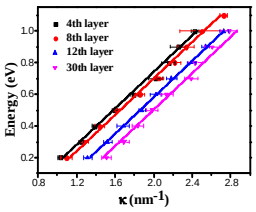

§ 2-3 扫描隧道谱的局限性和注意事项

微分电导(dI/dV)像的局限性：

恒定电流微分电导(dI/dV)像（STS at constant current）

将dI/dV随（x,y）的分布对应起来时，需要考虑到不同的形貌对于隧穿系数的影响。一般，对一个凸起的形貌，隧穿几率会偏小，而对于凹陷的形貌，隧穿几率会偏大。所以，dI/dV图事实上也是形貌和电子态密度的叠加。

dI/dV的零点发散问题：

对于接近于0的小偏压， dI/dV= I/V, 因此，对于一个固定的隧道电流，当V接近于零时，dI/dV是发散的，因此用此种方法不能获得费米能级附近的电子态密度。

电流成像隧道谱（Current imaging tunneling spectroscopy, CITS）

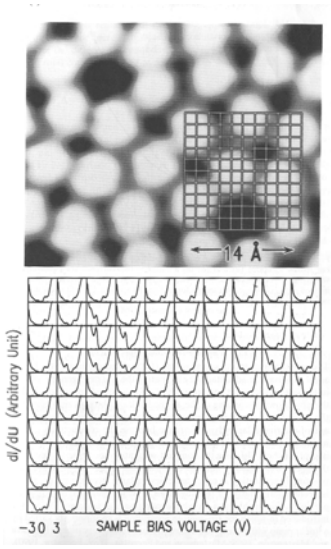

针对一张STM图上的每一个点，都分别采用测量固定高度单点微分电导*dI/dV*，以获得完整的dI/dV (x, y, V)图像。

获得的信息比恒定电流微分电导(dI/dV)像更加完整。并且不受零点发散问题的影响，可以获得费米能级附近的电子态信息。

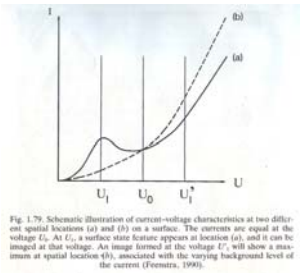

Fig. 1.79. Schematic illustration of current–voltage characteristics at two different spatial locations (a) and (b) on a surface. The currents are equal at the voltage U_0. At U_1, a surface state feature appears at location (a), and it can be imaged at that voltage. An image formed at the voltage U'_1 will show a maximum at spatial location (b), associated with the varying background level of the current (Feenstra, 1990).

电流成像隧道谱（Current imaging tunneling spectroscopy, CITS）

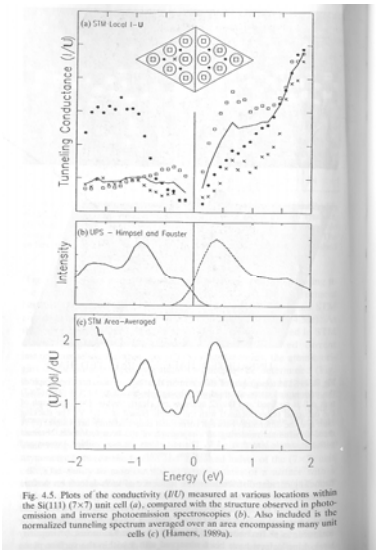

Fig. 4.5. Plots of the conductivity (*I/U*) measured at various locations within the Si(111) (7×7) unit cell (*a*), compared with the structure observed in photoemission and inverse photoemission spectroscopies (*b*). Also included is the normalized tunneling spectrum averaged over an area encompassing many unit cells (*c*) (Hamers, 1989a).

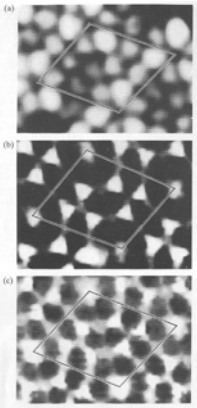

Fig. 4.6. CITS images of occupied Si(111) (7×7) surface states. (*a*) Adatom state at −0.35 V, (*b*) dangling-bond state at −0.8 V, (*c*) backbond state at −1.7 V (Hamers *et al.*, 1986a).

or as steps separating (111) terraces. The in-plane line defects appear as boundaries between translational domains of the (7×7) structure (Demuth *et al.*, 1986b; Berghaus *et al.*, 1988c; Köhler *et al.*, 1989; Sumita *et al.*, 1990; Hadley and Tear, 1991). These domain boundaries were found to play an essential role in the nucleation and growth behavior of the Si(111) 7×7 surface.

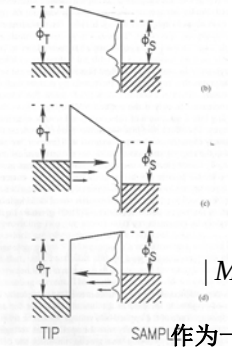

穿透系数随电压变化的影响

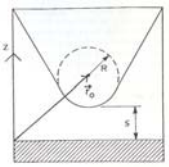

对于 kT～0时，一般情况：

$$I \propto \int_0^{eV} |M|^2 \rho_t(E)\rho_s(E+eV)dE$$

$$|M(V)|^2 \propto \exp\{-2(s+R)[\frac{2m}{\hbar^2}(\frac{\phi_t+\phi_s}{2}-\frac{|eV|}{2})^{1/2}]\}$$

作为一级近似可以认为dI/dV(V)对应样品的电子态密度函数。但是，实际上穿透系数作为偏压的函数，其变化也是很明显的。从物理图像上看，能量最高的电子（即施加负电压的电极一侧靠近费米能级附近的电子）具有最大的隧穿几率，贡献了大部分的电流。

通常，电压每增加一伏，由于穿透系数的增加而导致的电流增加一个数量级。但是，透射系数只是提供一个叠加在态密度变化函数上的单调递增的背景,并不影响电子态分布的结构。

通常对dI/dV谱进行归一化-> (dI/dV)/(I/V),部分消穿透系数的影响。

局限：STS能够准确反应样品的电子空态，但经常无法获得电子满态的信息？

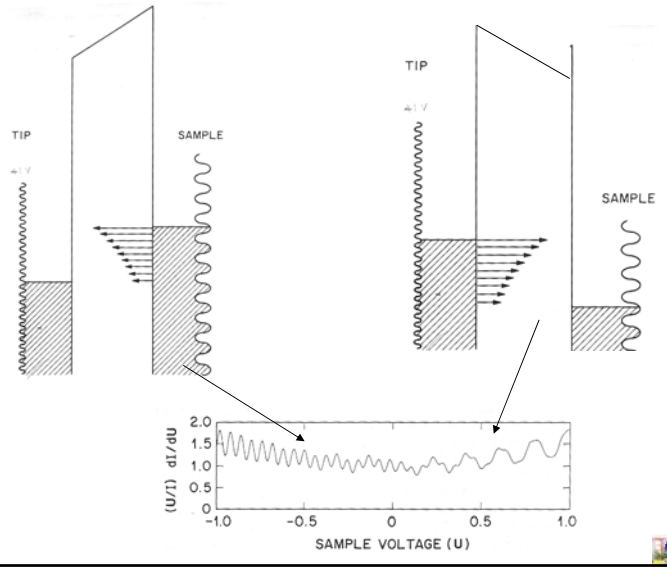

1-2 隧道电流谱的不同形式

1-2-4 功函数谱

$$I \propto \exp(-2\kappa s)$$

其中 $\kappa = (2m\phi)^{1/2}/\hbar$

其中 为有效局域势垒高度。Tersoff与Hamman认为 ϕ 在平面内是均一的，亦即与位置(x,y)无关。并且等于表面功函数。

$$\phi_A[\mathrm{eV}] = \frac{\hbar^2}{8m}\left(\frac{\mathrm{d}\ln I}{\mathrm{d}s}\right)^2 \approx 0.95\left(\frac{\mathrm{d}\ln I}{\mathrm{d}s\,[\text{Å}]}\right)^2$$

因此，测量 I-S曲线，即可以得到表面的平均功函数。

近场效应对功函数的影响

功函数的定义：将一个电子从固体的费米能级移到真空中所对应的能量。
功函数的来源：电子逸出效应和表面dipole。
对于针尖和样品距离比较远，针尖处于镜像电荷势场之外的情况，有效势垒可以近似地认为等于表面的平均功函数。但是，当针尖与表面的距离很近（5-10Å左右）时，针尖处在镜像电荷的势场中。故势垒与针尖和样品的距离有关。Bining提出一个一维模型：

$$\phi(d) = \phi_0 - \frac{\alpha}{d}$$

$\phi(d) = \phi_0 - \alpha / d$

其中$\phi_0 = (\phi_s + \phi_t)/2$为样品和针尖的平均功函数，$d$为针尖镜像平面与样品镜像平面的距离（与针尖和样品的距离略有不同，$d \approx s - 1.5$ Å

$$\frac{\mathrm{d}\ln I}{\mathrm{d}s} = -\frac{2(2m)^{1/2}}{\hbar}\cdot\phi_0^{1/2}\left[1+\frac{\alpha^2}{8\phi_0^2 d^2}+\mathcal{O}\left(\frac{1}{d^3}\right)\right]$$

$$\frac{d\ln I}{ds} = const$$

$$\phi_A \approx \phi_0 = const$$

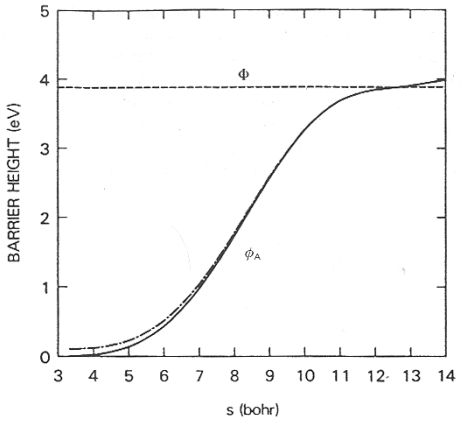

Fig. 1.73b. Apparent barrier height ϕ_A for two jellium electrodes, one representing the sample, the other, with an adsorbed Na atom, representing the tip. The work function ϕ for the sample electrode by itself is shown for comparison. The tip–sample separation is denoted by s (1 bohr = 0.529 Å) (Lang, 1988).

在**Z**陶瓷上加一个调制信号，调制针尖和样品的距离；用锁相放大器测量隧道电流的响应，根据上式就可以得到局域功函数。在扫描中进行测量，可以在得到形貌图的同时得到功函数象。

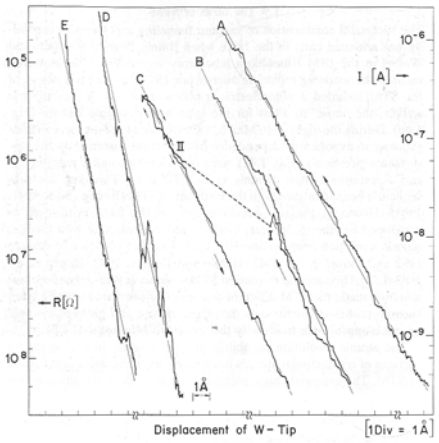

Fig. 1.41. Tunnel resistance and current versus displacement of a Pt sample with respect to the tip for different sample and tip conditions (Binnig *et al.*, 1982a).

隧道电流和针尖位置关系图，从中得到样品的功函数为**3.5eV**。

G. Binnig, et al, APL 40 (1982) 178